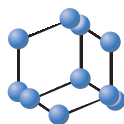


RESEARCH ARTICLE

BENTHAM
SCIENCE

CETP Inhibitory Activity of Chlorobenzyl Benzamides: QPLD Docking, Pharmacophore Mapping and Synthesis



Reema Abu Khalaf^{*}, Hamada Abd El-Aziz, Dima Sabbah, Ghadeer Albadawi and Ghassan Abu Sheikha

Department of Pharmacy, Faculty of Pharmacy, Al-Zaytoonah University of Jordan, Amman, Jordan

Abstract: Background: Elevated levels of serum LDL and total cholesterol are considered important risk factors for the development of atherosclerosis. Cholesteryl ester transfer protein inhibition raises HDL levels and reduces atherosclerotic lesions.

Objective: Consequently, there is a great interest in developing new CETP inhibitors.

Methods: Herein, synthesis of four chlorobenzyl benzamides **8a-d** that aim at CETP inhibition was performed.

Results: Benzamide **8a** showed the best CETP inhibitory activity with an IC_{50} of 1.6 μ M. *In vitro* biological data shows that the presence of *p*-trifluoromethoxy group enhances CETP inhibitory activity more than *m*-trifluoromethyl groups. QPLD docking shows that the verified compounds accommodate the binding cleft of CETP and are enclosed by hydrophobic lining. The scaffold of **8a-d** matches the pharmacophoric points of CETP inhibitors; particularly hydrophobic and aromatic functionalities.

Conclusion: Future structural modification is needed to improve CETP inhibitory activity and to enhance understanding of the structure-activity relationship.

Keywords: Atherosclerosis, CETP inhibitors, chlorobenzyl benzamides, docking, QPLD, pharmacophore mapping.

1. INTRODUCTION

Hyperlipidemia is characterized by abnormal lipid levels: higher levels of blood total cholesterol (TC), triglycerides (TG), and low density lipoprotein (LDL) cholesterol along with lower levels of high density lipoproteins (HDL) cholesterol [1]. The increased levels of serum LDL and TC are considered important risk factors for the development of atherosclerosis [2]. The elevation in serum levels of TC, TG and LDL, could be either alone or in combination [3, 4].

Cholesteryl ester transfer protein (CETP) is considered to be pro-atherogenic by lowering HDL and increasing LDL levels [5]. CETP inhibition increases HDL levels and reduces atherosclerotic lesions [6]. HDL has numerous properties that protect against atherosclerosis progress [7].

Plasma CETP is a hydrophobic glycoprotein that transfers lipids between HDL and apolipoprotein B-containing lipoproteins, and/or between HDL subparticles [8]. It facilitates the transfer of cholesteryl ester from the athero-

protective HDL to the proatherogenic LDL and VLDL. Epidemiologic studies support an inverse relation between HDL cholesterol and coronary heart disease [9]. Therefore, there has been a pronounced interest in developing new CETP inhibitors [10].

The crystal structure of CETP displays a long hydrophobic groove that comprises two molecules of cholesteryl ester and two phospholipid molecules [4]. CETP, the main key binding residues are hydrophobic and this concludes that hydrophobic binding interactions are dominating [11].

CETP inhibitors prevent the transfer of cholesteryl ester from HDL to VLDL and LDL, thus increasing HDL cholesterol and decreasing LDL cholesterol [12-14]. Several reported CETP inhibitors are undergoing clinical trials such as, dalcetrapib [15], anacetrapib [16], and evacetrapib [17].

Our research group identified different potential CETP inhibitors including benzylideneamino-methanones [18], benzylamino-methanones [19], *N*-(4-benzyloxyphenyl)-4-methyl-benzenesulfonamides, *N*-(4-benzylamino-phenyl)-toluene-4-sulfonic acid esters [20], and fluorinated benzamides [21].

In order to optimize the activity of our previously discovered popular compounds [19], hydrophobicity was enhanced

ARTICLE HISTORY

Received: January 07, 2017
Revised: March 21, 2017
Accepted: March 22, 2017

DOI:
10.2174/1570180814666170412122304

*Address correspondence to this author at the Department of Pharmacy, Faculty of Pharmacy, Al-Zaytoonah University of Jordan, Amman, Jordan; Tel: +962-64291511; Ext 239; Fax: 00962-64291432; E-mails: reema.abukhalaf@zuj.edu.jo and rима_abu_khalaf@yahoo.com

by an additional aromatic ring. Moreover, modifications of the linker groups together with the aromatic substitutions were carried out. These modifications led to the discovery of more hydrophobic molecules with greater CETP inhibition. This result matches with the hydrophobic nature of CETP binding pocket, and with the pharmacophore mapping and QPLD docking outcomes of the newly synthesized CETP inhibitors.

2. EXPERIMENTAL

2.1. Methods and Materials

All chemicals, reagents and solvents were of analytical grade and used directly without extra purification. Chemicals and solvents were purchased from the corresponding companies (Alfa Aesar, Acros Organics, Sigma-Aldrich, Fluka, SD fine Chem Limited, Tedia and Fisher Scientific).

Melting points were measured using Gallenkamp melting point apparatus and uncorrected. Infrared (IR) spectra were recorded using Shimadzu IR Affinity1 FTIR spectrophotometer. All samples were prepared with potassium bromide and pressed into a disc. ¹H-NMR and ¹³C-NMR spectra were measured on Bruker, Avance DPX-400 and Bruker 300 MHz-Avance III spectrometers, Jordan University of Science and Technology. Chemical shifts are given in δ (ppm) using TMS as the internal reference; the samples were dissolved in CDCl₃ or DMSO-d₆. High resolution mass spectrometry (HR-MS) was performed using LC Mass Bruker Apex-IV mass spectrometer utilizing an electrospray interface. AFLX800TBI Microplate Fluorimeter was used in the *in vitro* bioassay (BioTek Instruments, Winooski, VT, USA).

Thin Layer Chromatography (TLC) was performed on 20 x 20 cm layer with the thickness of 0.2 mm aluminum cards pre-coated with fluorescent silica gel GF254 DC- alufolienkieselgel (Fluka analytical, Germany), and visualized by UV light indicator (at 254 and/ or 360 nm).

2.2. Synthesis of the Compounds

2.2.1. General Procedure for the Synthesis of Methyl Benzoates Intermediates (5a, b)

3-Aminobenzoic acid (**1**, 2.0 g, 14.58 mmol) was dissolved in methanol (20 mL) and cooled down in the ice bath. The solution was treated with oxalyl chloride (**2**, 2.5 mL, 29 mmol) stirred at room temperature for 20-30 minutes, and refluxed for 24 hours at 60-70 °C. The reaction mixture was then evaporated and neutralized by 3M potassium carbonate. Extraction by chloroform (4 x 20 mL) was carried out four times. The organic layer was dried with sodium sulfate anhydrous followed by evaporation to get 2.07 g of pure 3-aminobenzoic acid methyl ester (**3**). Afterward, 3-aminobenzoic acid methyl ester (**3**, 2.0 g, 13.2 mmol) was dissolved in (20 mL) dichloromethane.

2.2.1.1. Methyl 3-(4-(trifluoromethoxy) benzylamino) benzoate (5a)

1-(bromomethyl)-4-(trifluoromethoxy) benzene (**4a**, 4.2 mL, 26.4 mmol), and triethylamine (9.2 mL, 66 mmol) were added to the solution of **3**. The mixture was left under stir-

ring at room temperature for 5 days then the mixture was evaporated. Column chromatography was carried out using cyclohexane: ethyl acetate (9:1) as eluent to afford **5a** as off white powder (2.18 g, 44%); m.p. 85-86°C; R_f = 0.46 (cyclohexane:ethyl acetate, 9:1); ¹H-NMR (300MHz, CDCl₃): δ 3.84 (s, 2H, NHCH₂), 4.63 (s, 3H, OCH₃), 6.83 (dd, J=4, 15 Hz, 1H, Ar-H), 7.20 (d, J=12 Hz, 2H, Ar-H), 7.22-7.25 (m, 4H, Ar-H), 7.40 (d, J=12 Hz, 1H, Ar-H), 7.44 ppm (s, 1H, NHCH₂); ¹³C-NMR (75MHz, CDCl₃): δ 53.6, 59.6, 113.4, 117.1, 118.7, 121.4, 128.1, 129.5, 136.5, 150.0, 168.0 ppm; IR (KBr): 3480, 3225, 2986, 1713, 1620, 1458, 1404, 1303, 1250 cm⁻¹.

2.2.1.2. Methyl 3-(3,5-bis(trifluoromethyl)benzyl) benzylamino benzoate (5b)

1-(bromomethyl)-3, 5-bis(trifluoromethyl) benzene (**4b**, 4.6 mL, 25 mmol), and triethylamine (8.76 mL, 62 mmol) were added to the solution of **3**. The mixture was left under stirring at room temperature for 7 days then the mixture was evaporated. Column chromatography was carried out using cyclohexane: ethyl acetate (8.5:1.5) as eluent to afford **5b** as yellow powder (1.34 g, 28%); m.p. 109-110 °C; R_f = 0.66 (chloroform, 10); ¹H-NMR (300MHz, CDCl₃): δ 3.86 (s, 3H, OCH₃), 4.33 (t, J=6 Hz, 1H, NHCH₂), 4.49 (d, J=6 Hz, 2H, HNCH₂), 6.73 (dd, J=3, 9 Hz, 1H, Ar-H), 7.19 (t, J=9 Hz, 1H, Ar-H), 7.29 (d, J=3 Hz, 1H, Ar-H), 7.40 (d, J=9 Hz, 1H, Ar-H), 7.82 ppm (d, J=12 Hz, 3H, Ar-H); ¹³C-NMR (75MHz, CDCl₃): δ 47.5, 52.1, 113.7, 117.4, 119.7, 121.4, 121.5, 121.6, 127.4, 129.5, 131.3, 142.0, 147.3, 168.0 ppm; IR (KBr): 3402, 2955, 1713, 1605, 1512, 1443, 1381, 1297 cm⁻¹.

2.2.2. General Procedure for the Synthesis of the Targeted Compounds (8a, b)

The intermediate methyl 3-(4-(trifluoromethoxy) benzylamino) benzoate (**5a**) was dissolved in 1M sodium hydroxide (5 mL) and refluxed overnight at 100 °C, then the reaction mixture was neutralized with 1M hydrochloric acid and extracted three times using chloroform (3 x 20 mL). The organic layer was dried using anhydrous sodium sulfate and evaporated.

Subsequently, the intermediate 3-(4-(trifluoromethoxy) benzylamino) benzoic acid (**6a**, 0.2 g, 0.64 mmol) was dissolved in 10 mL dichloromethane and oxalyl chloride (**2**, 0.11 mL, 1.28 mmol) was added. The reaction was left under stirring for 5 days at 50-60 °C. Later the reaction mixture was evaporated.

2.2.2.1. 3-{4-(Trifluoromethoxy-benzyl)-[3-(4-trifluoromethoxy-benzylamino)-benzoyl]-amino}-N-(4-chlorobenzyl)-benzamide (8a)

4-Chloro benzylamine (**7a**, 0.125 mL, 1.03 mmol) was added together with 5 mL of triethylamine and stirred at room temperature for 5 days. Then the crude product was purified by column chromatography using cyclohexane: ethyl acetate (5.9:4.1) as eluent to afford **8a** as off white powder (138.9 mg, 41%); m.p. 112-114°C; R_f = 0.36 (cyclohexane:ethyl acetate, 45:55); ¹H-NMR (400MHz, DMSO-d₆): δ 4.13 (d, J=4 Hz, 2H, NHCH₂), 4.46 (d, J=4 Hz, 2H, NHCH₂), 5.00 (s, 2H, NCH₂), 6.86 (d, J=8 Hz, 2H, Ar-H), 7.21 (d, J=8 Hz, 2H, Ar-H), 7.31-7.37 (m, 10H, Ar-H), 7.83-

7.90 (m, 2H, Ar-H), 9.13 (t, $J=4$ Hz, 1H, CONH), 9.27 ppm (t, $J=4$ Hz, 1H, CONH); ^{13}C -NMR (100MHz, DMSO- d_6): δ 42.0, 50.6, 62.5, 121.0, 126.2, 126.3, 128.1, 128.2, 129.1, 129.2, 130.2, 131.3, 135.1, 135.9, 137.1, 138.5, 140.4, 147.5, 163.0, 164.8, 165.1 ppm; IR (KBr): 3364, 3248, 3094, 2963, 2917, 1689, 1636, 1589, 1481, 1404, 1157, 1011 cm^{-1} ; HR-MS (ESI, positive mode) m/z $[M+\text{Na}]^+$ 652.10723 ($\text{C}_{31}\text{H}_{24}\text{Cl}_2\text{F}_3\text{N}_3\text{O}_4\text{Na}$ requires 652.10960).

2.2.2.2. 3- $\{$ (4-(Trifluoromethoxy-benzyl)- $\{$ 3-(4-trifluoromethoxy-benzylamino)-benzoyl $\}$ -amino $\}$ -N-(2-chlorobenzyl)-benzamide (8b)

2-Chloro benzylamine (**7b**, 0.125 mL, 1.03 mmol) was added together with 5 mL of triethylamine and stirred at room temperature for 5 days. Then the crude product was purified by column chromatography using cyclohexane: ethyl acetate (6.8:3.2) as eluent to afford **8b** as off white powder (42.5 mg, 21.3%); m.p. 91-93 $^\circ\text{C}$; R_f = 0.66 (cyclohexane:ethyl acetate, 45:55); ^1H -NMR (400MHz, DMSO- d_6): δ 4.21 (d, $J=4$ Hz, 2H, NHCH_2), 4.54 (d, $J=4$ Hz, 2H, NHCH_2), 5.03 (s, 2H, NCH_2), 6.72 (d, $J=8$ Hz, 2H, Ar-H), 7.10 (t, $J=8$ Hz, 2H, Ar-H), 7.21 (t, $J=8$ Hz, 2H, Ar-H), 7.29-7.47 (m, 8H, Ar-H), 7.87 (d, $J=8$ Hz, 2H, Ar-H), 9.07 (t, $J=4$ Hz, 1H, CONH), 9.30 ppm (t, $J=4$ Hz, 1H, CONH); ^{13}C -NMR (100MHz, DMSO- d_6): δ 40.5, 50.6, 61.8, 121.0, 126.5, 127.1, 127.3, 128.6, 128.7, 129.1, 129.8, 131.9, 132.0, 135.0, 135.8, 136.2, 140.5, 147.8, 163.7, 164.7, 165.4 ppm; IR (KBr): 3364, 3256, 3094, 2963, 2932, 1674, 1643, 1582, 1543, 1481, 1435, 1108, 1018 cm^{-1} ; HR-MS (ESI, positive mode) m/z $[M+\text{Na}]^+$ 652.10801 ($\text{C}_{31}\text{H}_{24}\text{Cl}_2\text{F}_3\text{N}_3\text{O}_4\text{Na}$ requires 652.10960).

2.2.3. General Procedure for the Synthesis of the Targeted Compounds (8c, d)

The intermediate methyl 3-(3,5-bis(trifluoromethyl) benzyl) benzylamino) benzoate (**5b**) was dissolved in 1M sodium hydroxide (5 mL) and refluxed overnight at 100 $^\circ\text{C}$, then the reaction mixture was neutralized with 1M hydrochloric acid and extracted three times using chloroform (3 x 20 mL). The organic layer was dried using anhydrous sodium sulfate and evaporated.

Subsequently, the intermediate 3-(3,5-bis (trifluoromethyl) benzylamino) benzoic acid (**6b**, 0.2 g, 0.64 mmol) was dissolved in 10 mL dichloromethane and oxalyl chloride (2, 0.1 mL, 1.1 mmol) was added. The reaction was left under stirring for 5 days at 50-60 $^\circ\text{C}$. Later the reaction mixture was evaporated.

2.2.3.1. 3- $\{$ (3,5-Bis(trifluoromethyl-benzyl)- $\{$ 3-(3,5-bis-trifluoromethyl-benzylamino)-benzoyl $\}$ -amino $\}$ -N-(4-chlorobenzyl)benzamide (8c)

4-Chloro benzylamine (**7a**, 0.1 mL, 0.89 mmol) was added together with 5 mL of triethylamine and stirred at room temperature for 5 days. Then the crude product was purified by column chromatography using cyclohexane: ethyl acetate (6:4) as eluent to afford **8c** as white powder (124 mg, 62%); m.p. 184-186 $^\circ\text{C}$; R_f = 0.46 (cyclohexane:ethyl acetate, 65:45); ^1H -NMR (400MHz, DMSO- d_6): δ 4.15 (d, $J=8$ Hz, 2H, NHCH_2), 4.45 (d, $J=8$ Hz, 2H, NHCH_2), 5.21 (s, 2H, NCH_2), 6.89 (d, $J=8$ Hz, 2H, Ar-H),

7.22 (d, $J=4$ Hz, 2H, Ar-H), 7.31-7.38 (m, 3H, Ar-H), 7.66-7.72 (m, 3H, Ar-H), 7.83 (d, $J=8$ Hz, 2H, Ar-H), 7.91 (s, 2H, Ar-H), 8.01 (s, 1H, Ar-H), 9.12 (t, $J=8$ Hz, 1H, CONH), 9.36 ppm (t, $J=8$ Hz, 1H, CONH); ^{13}C -NMR (100MHz, DMSO- d_6): δ 40.1, 50.1, 67.4, 123.6, 126.5, 127.4, 128.1, 128.2, 128.3, 128.7, 129.1, 131.6, 131.7, 135.3, 136.9, 141.0, 164.6, 166.8, 167.0 ppm; IR (KBr): 3341, 3240, 3086, 2963, 2932, 1674, 1628, 1551, 1497, 1381 cm^{-1} ; HR-MS (ESI, positive mode) m/z $[M+\text{Na}]^+$ 704.10144 ($\text{C}_{32}\text{H}_{23}\text{Cl}_2\text{F}_6\text{N}_3\text{O}_3\text{Na}$ requires 704.10206).

2.2.3.2. 3- $\{$ (3,5-Bis(trifluoromethyl-benzyl)- $\{$ 3-(3,5-bis-trifluoromethyl-benzylamino)-benzoyl $\}$ -amino $\}$ -N-(2-chlorobenzyl)benzamide (8d)

2-Chloro benzylamine (**7b**, 0.1 mL, 0.89 mmol) was added together with 5 mL of triethylamine and stirred at room temperature for 5 days. Then the crude product was purified by column chromatography using cyclohexane: ethyl acetate (7.6:2.4) as eluent to afford **8d** as white crystalline powder (103 mg, 51.5%); m.p. 158-160 $^\circ\text{C}$; R_f = 0.71 (cyclohexane:ethyl acetate, 55:45); ^1H -NMR (400MHz, DMSO- d_6): δ 4.24 (d, $J=4$ Hz, 2H, NHCH_2), 4.53 (d, $J=8$ Hz, 2H, NHCH_2), 5.24 (s, 2H, NCH_2), 6.77 (d, $J=8$ Hz, 1H, Ar-H), 7.11 (t, $J=8$ Hz, 1H, Ar-H), 7.19 (t, $J=8$ Hz, 1H, Ar-H), 7.30-7.46 (m, 7H, Ar-H), 7.86 (d, $J=8$ Hz, 2H, Ar-H), 7.92 (s, 2H, Ar-H), 8.02 (s, 1H, Ar-H), 9.07 (t, $J=4$ Hz, 1H, CONH), 9.38 ppm (t, $J=8$ Hz, 1H, CONH); ^{13}C -NMR (100MHz, DMSO- d_6): δ 40.6, 50.4, 66.6, 124.0, 126.6, 126.9, 127.1, 128.3, 128.5, 128.6, 128.7, 128.8, 129.0, 129.1, 132.0, 135.0, 136.2, 140.3, 165.0, 165.4, 167.2 ppm; IR (KBr): 3364, 3217, 3086, 2924, 1667, 1635, 1559, 1505, 1420, 1381 cm^{-1} ; HR-MS (ESI, positive mode) m/z $[M+\text{Na}]^+$ 704.10087 ($\text{C}_{32}\text{H}_{23}\text{Cl}_2\text{F}_6\text{N}_3\text{O}_3\text{Na}$ requires 704.10206).

2.3. Computational Methods

2.3.1. Preparation of Protein Structure

The X-ray crystal structure of cholesteryl ester transfer protein (CETP) (PDB ID: 4EWS) [11] was retrieved from the RCSB Protein Data Bank. The coordinates were prepared and energetically minimized using the Protein Preparation [22] wizard in the Schrödinger software suite to maximize H-bond interactions.

2.3.2. Preparation of Ligand Structure

The verified compounds (ligands) were built based on the coordinates of (ORP) in 4EWS [11]. The ligands were built using MAESTRO build panel and energy minimized by MacroModel [22] program using the OPLS2005 force field.

2.4. Quantum-Polarized Ligand Docking (QPLD)

QPLD [22] is a docking approach that recruits the combined quantum mechanical/ molecular mechanical (QM/MM) approach to determine ligand/protein interactions. The QPLD procedure starts with Glide [22] docking to generate a list of docked poses of a ligand that fit the protein binding cleft. The interaction energy of the protein/newly generated ligand pose is calculated while treating the protein with the MM method and the ligand pose with QM method employing the QSite program in Schrödinger [22]. The Qsite

program produces a new set of atomic partial charges for the ligand pose within the protein environment. The ligand poses with QM-generated partial charges are redocked to the binding site using Glide [22] program with XP-scoring function. QPLD takes into account the polarization effect of protein binding pocket during the docking process. And, the ligand pose with the lowest root mean square deviation is extracted. The binding site of the protein domain is determined using the ligand as a centroid. The Vander Waals scaling of the non-polar receptor atoms is set to 1.0.

2.5. Pharmacophore Mapping

Utilizing a previously generated pharmacophore model by our group [21], and in order to get further details about the functionalities of the synthesized compounds responsible for activity, **8a-d** were mapped against the adopted pharmacophore model of CETP inhibitors [21].

2.6. In Vitro CETP Inhibition Bioassay

An aliquot of rabbit serum (1.5 μ L) was mixed with 160 μ L of the tested sample. The donor and acceptor molecules in the assay buffer were added, mixed well, and the volume was adjusted to 203 μ L using the assay buffer.

Then, the mixture was incubated at 37°C for 1 hour. Fluorescence intensity (Excitation λ : 465 nm; Emission λ :

535 nm) was read using FLX800TBI Microplate Fluorimeter (BioTek Instruments, Winooski, VT, USA).

The synthesized molecules were dissolved in DMSO yielding 10 mM stock solutions. Next, dilution to the required concentration was attained using distilled deionized water. DMSO concentration was adjusted to 0.1%. CETP activity is not affected by DMSO. The percentage of residual CETP activity was identified in the presence and absence of the tested molecules.

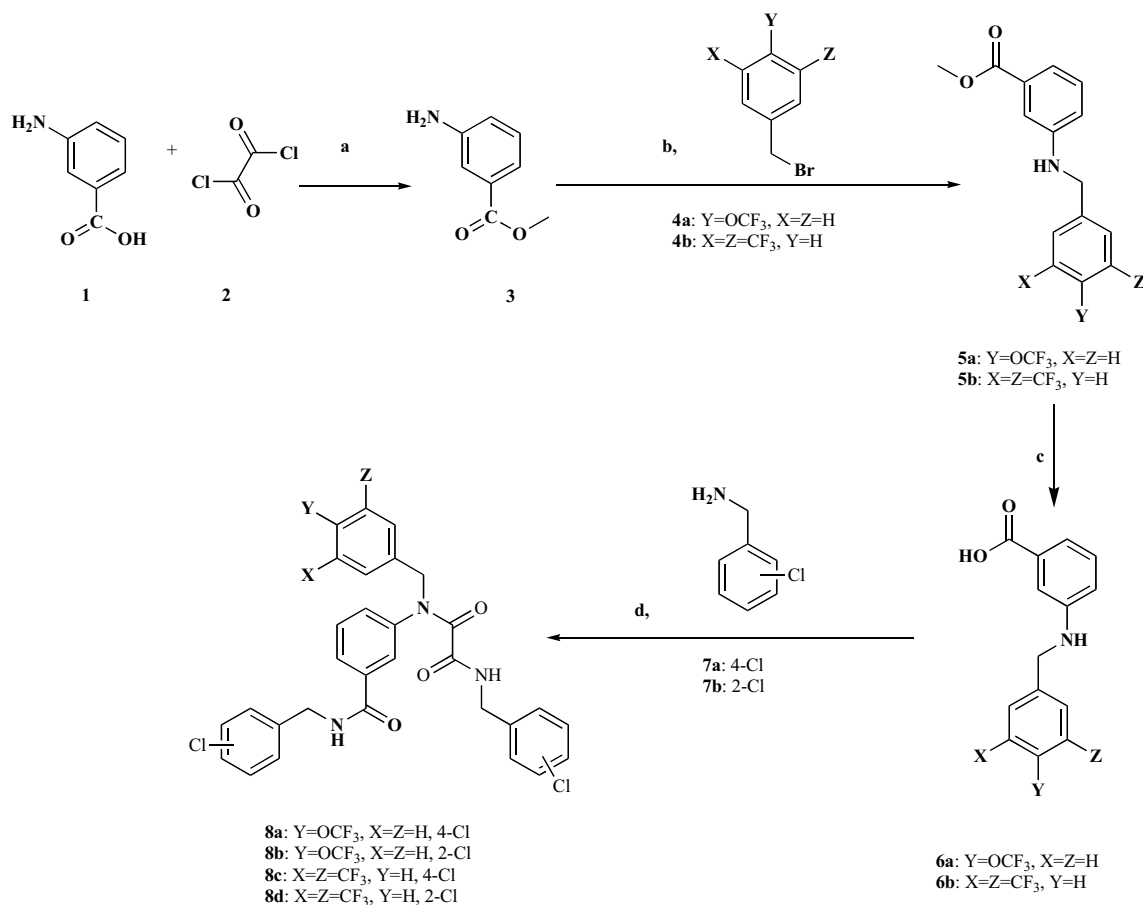
Negative control samples missing rabbit serum were used as a contrast background. Torcetrapib was used as a standard CETP inhibitor. The experimental protocol and measurements were carried out in duplicates. The % inhibition of CETP by the synthesized compounds was calculated using the following equation [18]:

$$\% \text{ Inhibition} = \left[1 - \frac{\text{Inhibitor read} - \text{Blank read}}{\text{Positive control} - \text{Negative control}} \right] * 100\%$$

3. RESULTS AND DISCUSSION

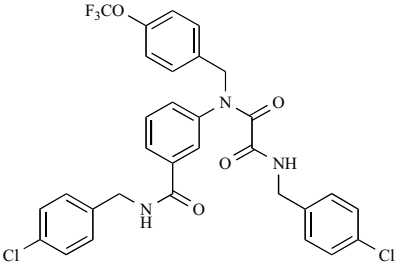
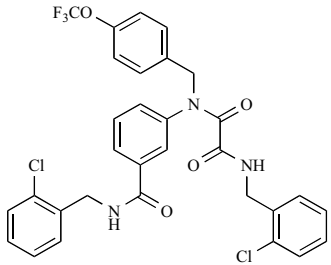
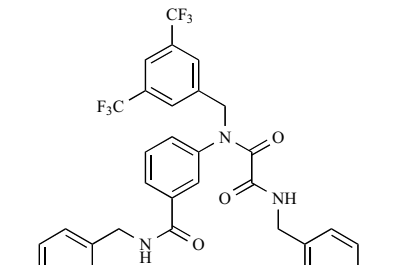
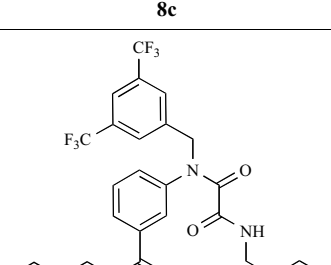
3.1. Chemistry

A series of chlorobenzyl benzamides **8a-d** were synthesized as shown in Scheme 1.



Scheme (1). Synthesis of chlorobenzyl benzamide derivatives **8a-d**. Reagents and conditions: (a) CH₃OH/reflux (60-70°C), 24 hours, (b) DCM, TEA, RT, 5 days, (c) (1) 1M NaOH (100°C), overnight, (2) 1M HCl, (d) (COCl)₂, TEA, DCM, RT, 5 days.

Table 1. *In vitro* bioactivities of synthesized chlorobenzyl benzamides 8a-d.

Compound	% Inhibition	IC ₅₀ (μM)
 <p>8a</p>	88.7 ^a	1.6
 <p>8b</p>	33.9 ^a	----
 <p>8c</p>	19.2 ^a	----
 <p>8d</p>	26.6 ^a	----
Torcetrapib	88.2 ^b	0.04

^aTested at 10 μM concentration.^bTested at 0.08 μM concentration.

The synthesis started with the activation of the carboxylic acid moiety of 3-aminobenzoic acid (**1**) using oxalyl chloride (**2**) in the presence of methanol to produce the corresponding methyl ester protecting group (**3**). Next, the amine nitrogen of 3-amino benzoic acid methyl ester (**3**) attacked the partially positive methylene group of the benzyl bromide (**4a, b**) in the presence of DCM as a solvent to produce substituted

3-benzylaminobenzoic acid methyl ester intermediates (**5a, b**). Triethylamine was used as an acid scavenger.

It was found that **5a** (44% yield) was produced in higher yield than **5b** (28%). Afterward, deprotection of the carboxylic acid group of 3-aminobenzoic acid methyl ester intermediates (**5a, b**) was carried out by alkaline hydrolysis using

1M NaOH under reflux followed by neutralization with 1M HCl. Again, activation of the carboxylic acid moiety of 3-benzylamino benzoic acid intermediates (**6a**, **b**) was performed using oxalyl chloride (**2**) to produce the corresponding acyl chloride derivatives in the presence of TEA and DCM. Additionally, oxalyl chloride reacted with the amine moiety of 3-benzylamino benzoic acid intermediates (**6a**, **b**). Subsequently, amide formation was attained by the nucleophilic attack of the amine moiety of chloro-benzylamine (**7a**, **b**) on the partially positive carbonyl carbon of the previously produced benzoyl chloride and acyl chloride to get the targeted chlorobenzyl benzamide derivatives **8a-d**.

The best yield was obtained upon reacting intermediate **6b** with 4-chloro benzylamine (**7a**) to produce **8c** in 62% yield. It is obvious that lower yield was achieved when using 2-chloro benzylamine (**7b**) which can be attributed to steric effect.

3.2. In Vitro CETP Inhibition Bioassay

The results of CETP inhibition bioassay, presented in Table 1, demonstrate that compound **8a** exhibit good activity against CETP with a percent inhibition of 88.7% at 10 μ M concentration and an IC_{50} of 1.6 μ M.

By comparing the structure of the synthesized compounds **8a-d** with their activities (Scheme 1, Table 1), it appears that the presence of the trifluoromethoxy group at the para position (as in compounds **8a** and **8b**) gives greater inhibitory activity than the two trifluoromethyl groups at the meta positions (as in compounds **8c** and **8d**).

On the other hand, it looks that the position of the chlorine substituent whether at the ortho or para position has greater influence on the CETP inhibitory activity of the synthesized compound when the structure is substituted with 4-trifluoromethoxy group rather than 3,5-difluoromethyl moieties.

3.3. Computational Results

3.3.1. Quantum-Polarized Ligand Docking (QPLD)

In order to determine the structural basis of binding of the synthesized compounds in 4EWS, QPLD was applied against 4EWS [23]. Cho *et al.* illustrated that incorporating the derived charges of quantum mechanical/molecular mechanical (QM/MM) approach into molecular docking significantly improved the predictive outcome of a docking program [24]. Our QPLD docking data for **8a-d** (Scheme 1) and ORP demonstrate that these compounds bind to the active domain of 4EWS. Interestingly, the hydrophobic interactions between the backbone of the binding site and the compounds' scaffold drive the activity (Fig. 1).

The fact that our verified molecules **8a-d** harbor four aromatic rings clarifies the dominance of hydrophobic (van der Waals) interactions (Fig. 2). Table 2 shows the QPLD docking scores of the synthesized compounds **8a-d** and ORP against 4EWS. The more the negative the docking score the better the binder. The fact that our compounds harbor four aromatic rings and other functionalities explains their higher binding scores compared to that of ORP. The absence of

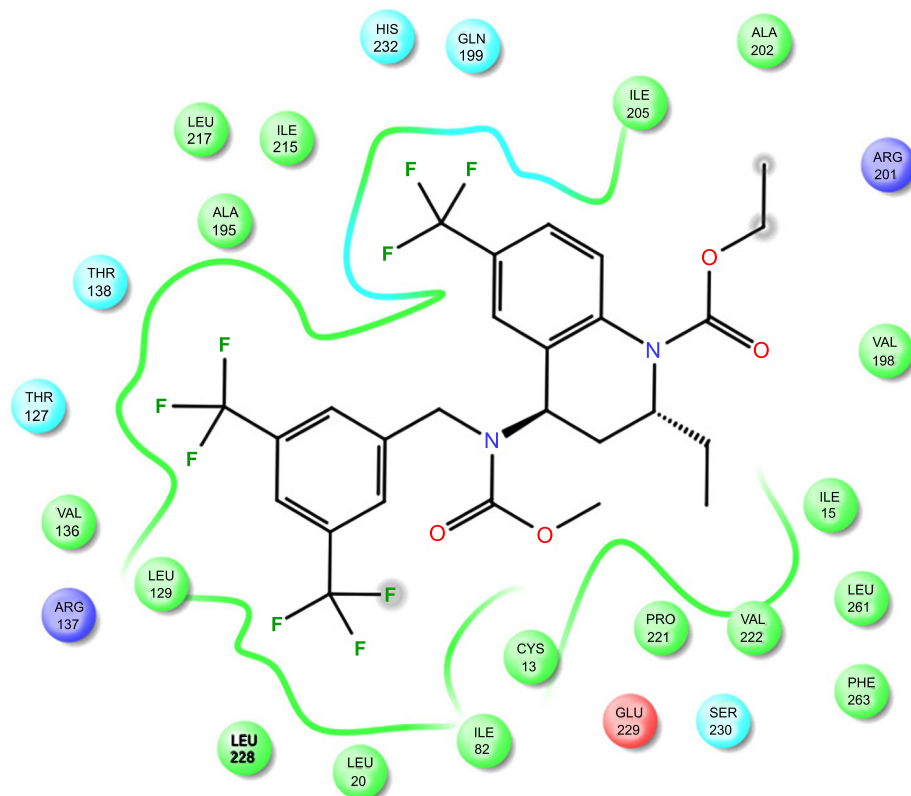


Fig. (1). The ORP/protein interaction. The hydrophobic lining depicted in green dominates the binding interaction. (The color version of the figure is available in the electronic copy of the article).

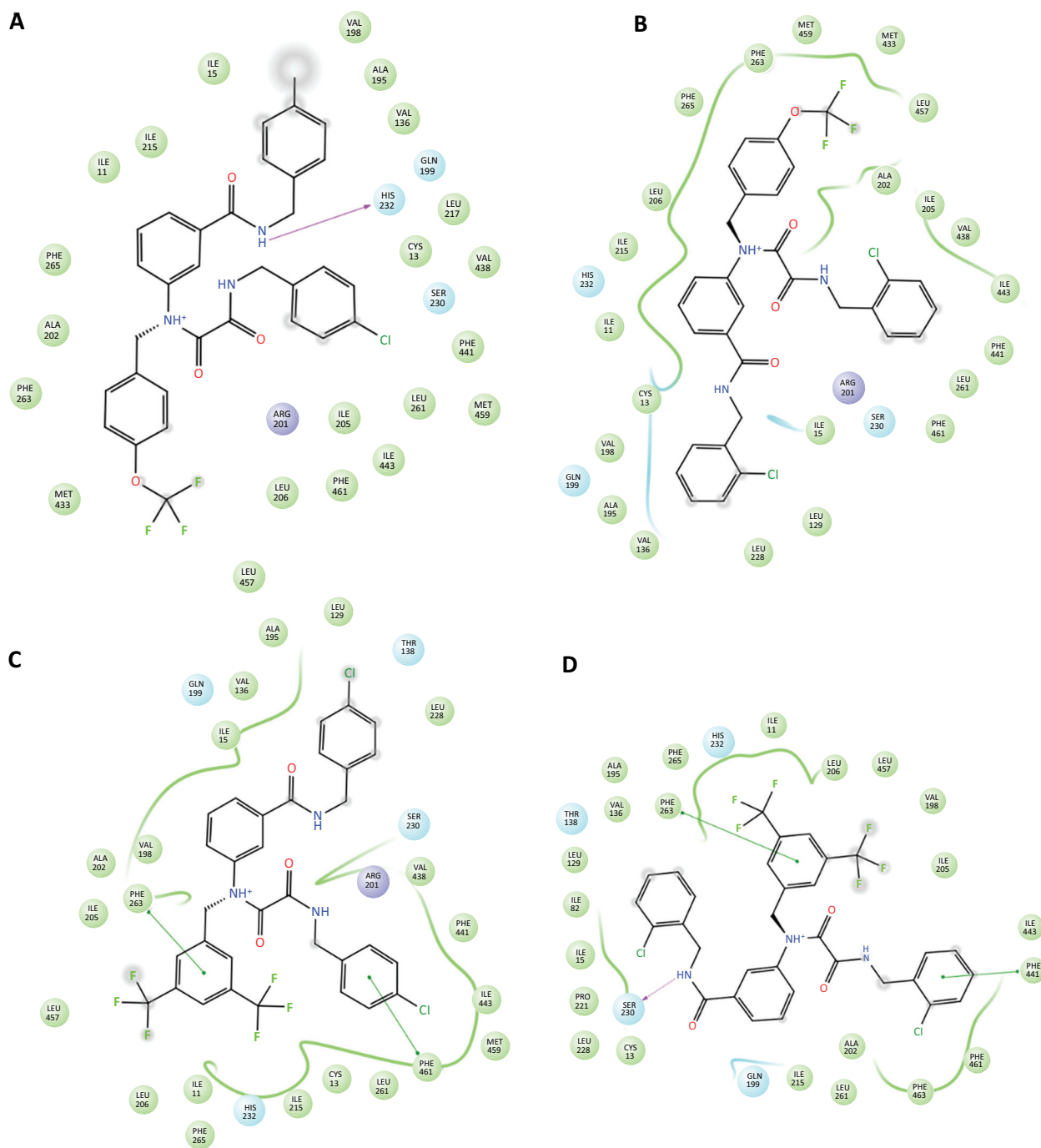


Fig. (2). The ligand/protein complex of (A) **8a**, (B) **8b**, (C) **8c** and (D) **8d**.

Table 2. The QPLD docking scores (Kcal/mol) of the verified compounds.

Compound	QPLD Docking Score (Kcal/mol)	H-bond	RMSD (Å)
ORP	-7.52	NA	1.950
8a	-11.44	H232	0.049
8b	-10.30	NA	0.002
8c	-9.44	NA	0.027
8d	-11.16	NA	0.033

NA: Not available

RMSD: Root mean square deviation of the re-docked position and the original position for ORP into 4EWS.

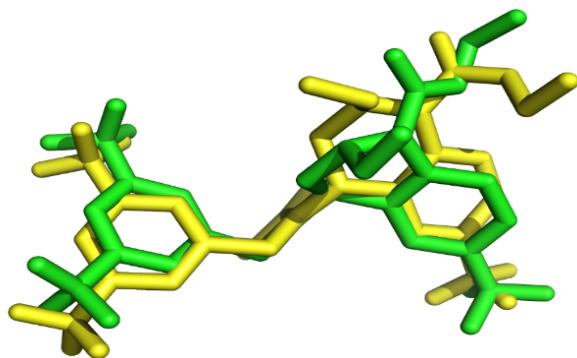


Fig. (3). The superposition of the QPLD-docked pose of ORP and its native conformation in 4EWS. The native coordinates are yellow colored and the docked pose is green colored. Picture made by PYMOL. (The color version of the figure is available in the electronic copy of the article).

H-bond interaction and the dominance of hydrophobic interaction is observed.

The docking scores for **8a-d** compared to ORP confirms that the more the attaching moieties the more the interaction. The *in vitro* biological data illustrates that **8a** is the most active derivative of this series followed by **8b**. Compounds **8c** and **8d** having aromatic rings tailored with two $-CF_3$ moieties showed less CETP inhibition. This confirms that the bulkiness of these compounds hinders their proper orientation in the binding domain and thus in turn decreases their activity.

3.4. Validation of the QPLD

In order to assess the QPLD performance, the docked pose of ORP in 4EWS was compared to its native conformation in the crystal structure. As can be seen in Fig. (3), there is a superposition of the QPLD-generated ORP pose and the native conformation in 4EWS. The RMSD for heavy atoms of ORP between the native poses and QPLD-generated docked poses was 1.950 Å, which designates the ability of QPLD docking to recognize the native poses in crystal structures and to effectively predict the ligand binding conformation.

3.5. Pharmacophore Mapping

In order to gain insight about the functionalities of the synthesized compounds, **8a-d** were screened against an adopted pharmacophore model [21] of CETP inhibitors (Fig. 4). The pharmacophore model demonstrates that the CETP inhibitor should harbor two aromatic (π -ring) or hydrophobic moieties (F1 and F2); three hydrophobic functionalities (F4, F5, and F6); two H-bond acceptors (F2 and F6); H-bond donor or cationic center (F6) to incite an activity [21].

The verified compounds matched the CETP inhibitors pharmacophoric features (Fig. 5). This describes the affinity of the targeted compounds toward CETP active domain. Furthermore, the accommodation of **8a-d** in the active binding site could explain their inhibitory activity.

The physicochemical properties of the synthesized molecules such as high molecular weight, number of aromatic rings, and log P violate Lipinski's rule of five [25, 26].

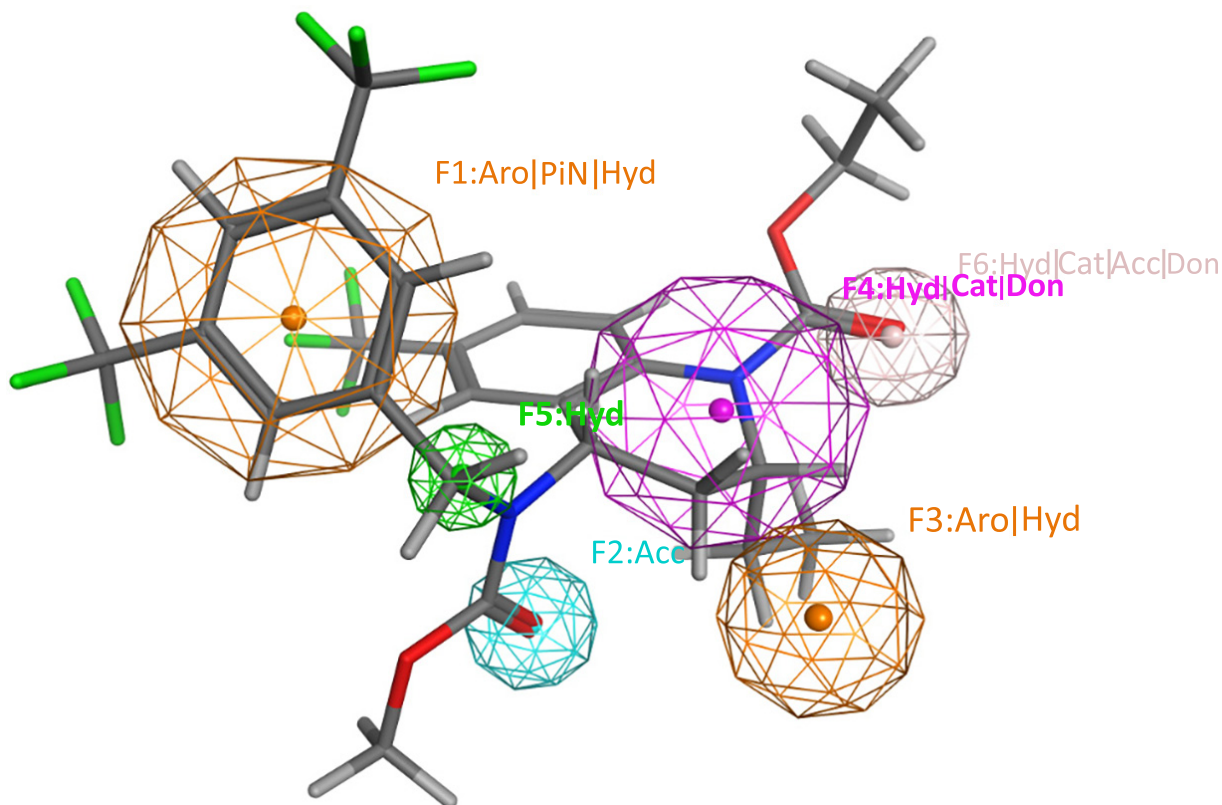


Fig. (4). Pharmacophore model of CETP inhibitor [21] with ORP. Aro stands for aromatic rings; Acc for H-bond acceptor; Don for H-bond donor; Cat for cationic group; PiN for π -ring; and Hyd for hydrophobic groups. Picture made by MOE [24].

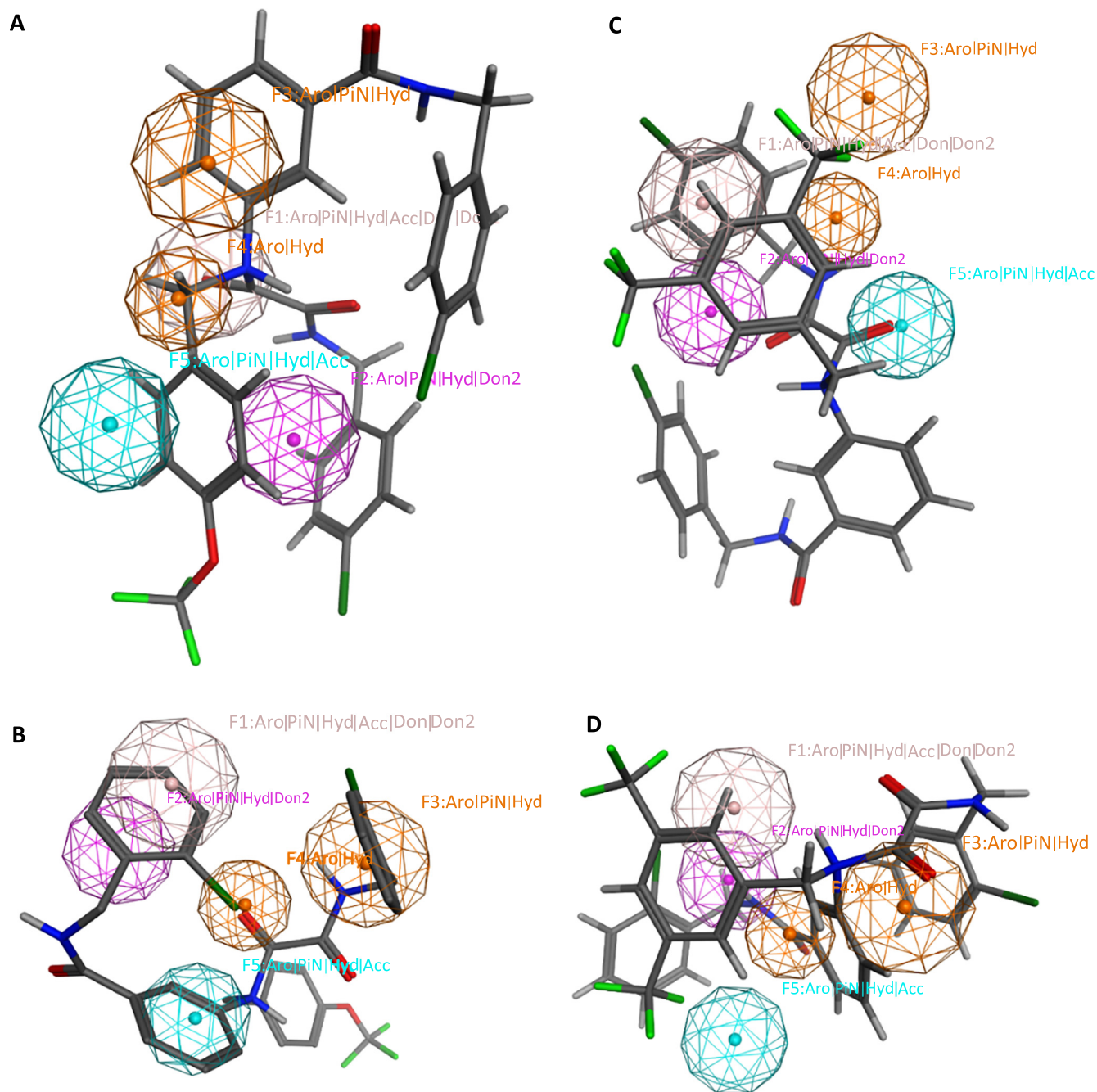


Fig. (5). Pharmacophore model of CETP inhibitor with (A) **8a**, (B) **8b**, (C) **8c**, and (D) **8d**.

Therefore, further optimization of this core nucleus is highly required to improve their physicochemical properties and better understand their structure-activity relationship.

CONCLUSION

This work identified chlorobenzyl benzamides as a new scaffold targeting CETP activity. Benzamide **8a** showed the highest inhibitory activity with an IC_{50} of 1.6 μ M. The study found that the presence of *p*-trifluoromethoxy (as in **8a**, **8b**) enhances CETP inhibitory activity more than *m*-trifluoromethyl groups (as in **8c**, **8d**).

The QPLD docking shows that compounds **8a-d** accommodate the binding cleft of CETP and the hydrophobic interaction mediates ligand/complex formation. The scaffold of **8a-d** matches the pharmacophoric points of CETP inhibitors; particularly hydrophobic and aromatic functionalities. The *in vitro* biological data shows that **8a** is the most potent derivative of this series followed by **8b**. The bulkiness of **8c** and **8d** having aromatic rings tailored with two $-CF_3$ moieties decreases their activity. This confirms that the bulkiness of these compounds impedes their proper orientation in the binding domain. Consequently, optimization of their struc-

ture is recommended to enhance their physicochemical properties and clarify their structure-activity relationship.

CONSENT FOR PUBLICATION

Not applicable.

CONFLICT OF INTEREST

The authors declare no conflict of interest, financial or otherwise.

ACKNOWLEDGEMENTS

The authors acknowledge the Scientific Research and Postgraduate Deanship at Al-Zaytoonah University of Jordan for sponsoring this project.

REFERENCES

- Choudhary, M.; Naheed, S.; Jalil, S.; Alam, J.; Attaur, R. Effects of ethanolic extract of iris germanica on lipid profile of rats fed on a high-fat diet. *J. Ethnopharmacol.*, **2005**, *98*, 217-220.
- Jang, A.; Srinivasan, P.; Lee, N.; Song, H.; Lee, J.; Lee, M.; Jo, C. Comparison of hypolipidemic activity of synthetic gallic acid-linoleic acid ester with mixture of gallic acid and linoleic acid gallic acid, and linoleic acid on high-fat diet induced obesity in C57bl/6 CR SLC mice. *Chem. Biol. Interact.*, **2008**, *174*, 109-117.
- Kosteva, K.; Wood, D.; De, B.G. Management of cardiovascular risk factors in asymptomatic high-risk patients in general practice: Cross-sectional survey in 12 European countries. *Eur. J. Cardiovasc. Prev. Rehabil.*, **2010**, *17*(5), 530-540.
- MacMahon, Z.; Wierzbicki, A. Lipid-lowering therapies: A prescribing guide. *Nurse Prescrib.*, **2011**, *9*(4), 180-188.
- Yamashita, S.; Hirano, K.; Sakai, N.; Matsuzawa, Y. Molecular biology and pathophysiological aspects of plasma cholesteryl ester transfer protein. *Biochim. Biophys. Acta*, **2000**, *1529*, 257-275.
- Okamoto, H.; Yonemori, F.; Wakitani, K.; Minowa, T.; Maeda, K.; Shinkai, H. A cholesteryl ester transfer protein inhibitor attenuates atherosclerosis in rabbits. *Nature*, **2000**, *406*, 203-207.
- Rye, K.; Bursill, C.; Lambert, G.; Tabet, F.; Barter, P. The metabolism and anti-atherogenic properties of HDL. *J. Lipid Res.*, **2009**, *50*, 195-200.
- Maugeais, C.; Perez, A.; von der Mark, E.; Magg, C.; Pflieger, P.; Niesor, E. Evidence for a role of CETP in HDL remodeling and cholesterol efflux: Role of cysteine 13 of CETP. *Biochim. Biophys. Acta*, **2013**, *183*, 1644-1650.
- Chapman, M.J.; Assmann, G.; Fruchart, J.-C.; Shepherd, J.; Sirtori, C. Raising high-density lipoprotein cholesterol with reduction of cardiovascular risk: The role of nicotinic acid - a position paper developed by the European consensus panel on HDL-C. *Curr. Med. Res. Opin.*, **2004**, *20*(8), 1253-1268.
- Kallashi, F.; Dooseop, K.; Kowalchick, J.; Park, Y.J.; Hunt, J.A.; Ali, A.; Smith, C.J.; Hammond, M.L.; Pivnichny, J.V.; Tong, X.; Xu, S.S.; Anderson, M.S.; Chen, Y.; Eveland, S.S.; Guo, Q.; Hyland, S.A.; Milot, D.P.; Cumiskey, A.-M.; Latham, M.; Peterson, L. B.; Rosa, R.; Sparrow, C.P.; Wright, S.D.; Sinclair, P.J. 2-Arylbezoxazoles as CETP inhibitors: Raising HDL-C in cyno CETP transgenic mice. *Bioorg. Med. Chem. Lett.*, **2011**, *21*(1), 558-561.
- Liu, S.; Mistry A Fau-Reynolds, J.M.; Reynolds Jm Fau-Loyd, D. B.; Loyd Db Fau-Griffor, M.C.; Griffor Mc Fau-Perry, D.A.; Perry Da Fau-Ruggeri, R.B.; Ruggeri Rb Fau-Clark, R.W.; Clark Rw Fau-Qiu, X.; Qiu, X. Crystal structures of cholesteryl ester transfer protein in complex with inhibitors. *J. Biol. Chem.*, **2012**, *287*, 37321-37329.
- Dong, B.; Singh, A.; Fung, C.; Kan, K.; Liu, J. CETP inhibitors down regulate hepatic LDL receptor and PCSK9 expression *in vitro* and *in vivo* through a SREBP@ dependent mechanism. *Atherosclerosis*, **2014**, *215*, 449-462.
- Johns, D.G.; Chen, Y.; Wang, S.-P.; Castro-Perez, J.; Previs, S.F.; Roddy, T.P. Inhibition of cholesteryl ester transfer protein increases cholesteryl ester content of large HDL independently of HDL-to-HDL homotypic transfer: *In vitro* vs *in vivo* comparison using anacetrapib and dalcetrapib. *Eur. J. Pharmacol.*, **2015**, *762*, 256-262.
- Schaefer, E.J. Effects of cholesteryl ester transfer protein inhibitors on human lipoprotein metabolism: why have they failed in lowering coronary heart disease risk? *Curr. Opin. Lipidol.*, **2013**, *24*(3), 259-264.
- Kuivenhoven, J.; de Grooth, G.; Kawamura, H.; Klerkx, A.; Wilhelm, F.; Trip, M.; Kastelein, J. Effectiveness of Inhibition of cholesteryl ester transfer protein by JTT-705 in combination with pravastatin in type II dyslipidemia. *Am. J. Cardiol.*, **2005**, *95*, 1085-1088.
- Cannon, C.; Shah, S.; Dansky, H.; Davidson, M.; Brinton, E.; Gotto, A.; Stepanavage, M.; Liu, S.; Gibbons, P.; Ashraf, T.; Zafarino, J.; Mitchel, Y.; Barter, P. Safety of anacetrapib in patients with or at high risk for coronary heart disease. *N. Engl. J. Med.*, **2010**, *363*, 2406-2415.
- Cao, G.; Beyer, T.; Zhang, Y.; Schmidt, R.; Chen, Y.; Cockerham, S.; Zimmerman, K.; Karathanasis, S.; Cannady, E.; Fields, T.; Mantlo, N. Evacetrapib is a novel, potent, and selective inhibitor of cholesteryl ester transfer protein that elevates HDL cholesterol without inducing aldosterone or increasing blood pressure. *J. Lipid Res.*, **2011**, *52*, 2169-2176.
- Abu Khalaf, R.; Abu Sheikha, G.; Bustanji, Y.; Taha, M. Discovery of new cholesteryl ester transfer protein inhibitors *via* ligand-based pharmacophore modeling and QSAR Analysis followed by synthetic exploration. *Eur. J. Med. Chem.*, **2010**, *45*(4), 1598-1617.
- Abu Sheikha, G.; Abu Khalaf, R.; Melhem, A.; Albadawi, G. Design, Synthesis and biological evaluation of benzylamino-methanone based cholesteryl ester transfer protein inhibitors. *Molecules*, **2010**, *15*(8), 5721-5733.
- Abu Khalaf, R.; Abu Sheikha, G.; Alsh'er, M.; Albadawi, G.; Taha, M. Design, synthesis and biological evaluation of benzenesulfonamide derivatives as potential CETP inhibitors. *Med. Chem. Res.*, **2012**, *21*(11), 3669-3680.
- Abu Khalaf, R.; Al-Rawasdeh, S.; Sabbah, D.; Abu Sheikha, G. Molecular docking and pharmacophore modeling studies of fluorinated benzamides as potential CETP inhibitors. *Med. Chem.*, **2017**, *3*(3), 239-253.
- Protein Preparation Wizard, M. Macromodel, and QPLD-dock, Schrödinger, LLC, Portland, OR, USA, **2016**.
- Cho, A.E.; Guallar, V.; Berne, B.J.; Friesner, R. Importance of accurate charges in molecular docking: Quantum mechanical/molecular mechanical (QM/MM) approach. *J. Comput. Chem.*, **2005**, *26*, 915-931.
- The Molecular Operating E.; Chemical Computing Group, I.; Montreal, Q.C. **2009**.
- Lipinski, C.A.; Lombardo, F.; Dominy, B.W.; Feeney, P.J. Experimental and computational approaches to estimate solubility and permeability in drug discovery and development settings. *Adv. Drug Delivery Rev.*, **1997**, *23*, 3-25.
- Lipinski, C.A.; Lombardo, F.; Dominy, B.W.; Feeney, P.J. Experimental and computational approaches to estimate solubility and permeability in drug discovery and development settings. *Adv. Drug Deliv. Rev.*, **2001**, *46*, 3-26.